

3D hydrodynamical model atmospheres: a tool to correct radial velocities and parallaxes for Gaia.

A. Chiavassa¹, L. Bigot², F. Thévenin², R. Collet³, G. Jasiewicz⁴, Z. Magic³, M. Asplund³

¹ Institut d'Astronomie et d'Astrophysique, Université Libre de Bruxelles, CP. 226, Boulevard du Triomphe, B-1050 Bruxelles, Belgium

² Université de Nice Sophia-antipolis, CNRS Laboratoire Cassiopée, Observatoire de la Côte d'Azur, B.P. 4229, 06304 Nice Cedex 4, France

³ Max-Planck-Institut für Astrophysik, Karl-Schwarzschild-Str. 1, Postfach 1317, D-85741 Garching b. München, Germany

⁴ LUPM, Laboratoire Univers et Particules, Université de Montpellier II, CNRS, Place Eugène Bataillon, 34095 Montpellier Cedex 05, France

E-mail: achiavas@ulb.ac.be

Abstract. Convection plays an essential role in the emerging intensity for many stars that will be observed by Gaia. Convective-related surface structures affect the shape, shift, and asymmetry of absorption lines, the photocentric and photometric variability causing bias in Gaia measurements. Regarding the importance of Gaia mission and its goals, it is mandatory to have the best models of the observed stars. 3D time-dependent hydrodynamical simulations of surface convection are crucial to model the photosphere of late type stars in a very realistic way. These simulations are an important tool to correct the radial velocities and better estimates the parallaxes and photometric variability.

1. Introduction

The main goal of the Gaia mission [1, 2] is to determine high-precision astrometric parameters (i.e., positions, parallaxes, and proper motions) for one billion objects with apparent magnitudes in the range $5.6 \leq V \leq 20$ and kinematic velocities of about 100 millions of stars with a precision of $\sim 1 \text{ km.s}^{-1}$ up to $V \leq 13$. These data along with multi-band and multi-epoch photometric data will allow to reconstruct the formation history, structure, and evolution of the Galaxy.

Convection plays a crucial role in the formation of spectral lines and deeply influences the shape, shift, and asymmetries of lines in late type stars which will represent most of the objects that will be observed by Gaia. In addition to this, granulation-related variability that is considered as "noise" must be quantified in order to better characterize any resulting systematic error on the parallax and photometric determinations.

Realistic modelling of stellar atmospheres is therefore crucial for a better interpretation of future Gaia data and, in this context, three-dimensional radiative-hydrodynamical models are needed for a quantitative correction of the radial velocities (few hundreds km.s^{-1}) for all the stars observed and, in evolved stars, for the determination of the photocenter positions.

2. Surface convection simulations and radiative transfer calculations

We adopted here time-dependent, three-dimensional (3D), radiative-hydrodynamical (RHD) surface convection simulations of different stars across the Hertzsprung-Russell diagram (Tab. 1). The simulations have been carried out using:

- The BOX-IN-A-STAR setup with STAGGER-CODE¹. These models cover only a small section of the surface layers atop the deep convection zone, and the numerical box includes a number of convective cells proportional to the surface gravity. They have constant gravity, the lateral boundaries are periodic, and the radiation transport module relies on a Feautrier scheme applied to long characteristics.
- The STAR-IN-A-BOX setup with CO⁵BOLD code [3, 4, 5]. These simulations cover the whole convective envelope of the star and have been used to model red supergiant (RSG) stars [3, 5] and Asymptotic giant branch stars [4] so far. The computational domain is an equidistant cubic grid in all directions, and the same open boundary condition is employed for all side of the computational box.

The transition between the box-in-a-star and star-in-a-box occurs around $\log g \sim 1$, when the influence of sphericity and the ratio between granule size versus stellar diameter become important; the star-in-a-box global models are then needed, but those are highly computer-time demanding and difficult to run so that there are only very few models available so far.

We used the 3D pure-LTE radiative transfer code OPTIM3D [6] to compute spectra and intensity maps from the snapshots of the RHD simulations listed in Table 1. The code takes into account the Doppler shifts due to convective motions. The radiative transfer equation is solved monochromatically using extinction coefficients pre-tabulated with the same chemical compositions as the RHD simulations and using the same extensive atomic and molecular opacity data as the latest generation of MARCS models [7]. We assumed a zero micro-turbulence since the velocity fields inherent in 3D models are expected to self-consistently and adequately account for non-thermal Doppler broadening of spectral lines.

3. Kinematic radial velocities and correction of convective shifts

A convenient and usual way to estimate kinematic radial velocity of a star is commonly made from a measurement of its spectroscopic radial velocity. Gaia is provided with a dedicated radial velocity spectrometer (RVS, [11]) with a resolving power at best of 11 500 centered on Ca II triplet in the spectral band from 8480 to 8750 Å. It is well known that photospheric absorption lines in many stars are blueshifted as a result of convective motions in the stellar atmosphere. In fact, hot bright and rising (i.e., blueshifted) convective elements contribute with more photons than cool dark shrinking gas: as a consequence, the absorption lines appear blueshifted [12, 13]. This effect is one of the systematic errors of spectroscopic measurements with RVS [14, 15] and will be taken into account by the analysis pipeline of Gaia using 3D RHD simulations [16], which naturally account for turbulent motions and therefore do not need the use of the traditional micro and macro turbulence used in hydrostatic models.

We computed synthetic spectra in RVS domain using OPTIM3D for all the models reported in Tab. 1. The spectra were computed along rays of four μ -angles [0.88, 0.65, 0.55, 0.34] and four ϕ -angles [0°, 90°, 180°, 270°], after which we performed a disk integration and a temporal average over all selected snapshots. It is important that the total time covered by the simulations is such that there are no trends in the lineshift if a subset of snapshots is used for the calculations. This has been verified by [17] for the simulation with $T_{\text{eff}}=4630$ and $\log g=1.6$ in

¹ www.astro.ku.dk/~aake/papers/95.ps.gz

Table 1. 3D hydrodynamical model atmospheres used in this work. The symbols refer to Fig. 5, 6, 7, and 8.

Stellar type	T_{eff} [K]	$\log g$	[Fe/H]	Mass [M_{\odot}]	R_{\star} [R_{\odot}]	$\Delta\lambda_{\text{FeI}}$ [km.s $^{-1}$]	$\Delta\lambda_{\text{CaII}}$ [km.s $^{-1}$]	Ref.	Symbol
Local simulations with STAGGER-CODE									
K giant	4700	2.2	0.0	-0.36	+0.29	[8]	●
K giant	4720	2.2	-1.0	-0.45	+0.23	[8]	▲
K giant	5035	2.2	-2.0	-0.58	+0.25	[8]	▼
K giant	5130	2.2	-3.0	-0.28	+0.31	[8]	◆
K giant	4630	1.6	-3.0	-0.22	+1.55	[9]	■
F star	6500	4.0	0.0	-0.75	+3.4	[10]	★
Global simulations with CO ⁵ BOLD									
RSG	3430	-0.35	0.0	12	846	+0.75	-1.89	[5]	●
RSG	3660	0.02	0.0	6	386	+2.80	-7.95	[5]	★

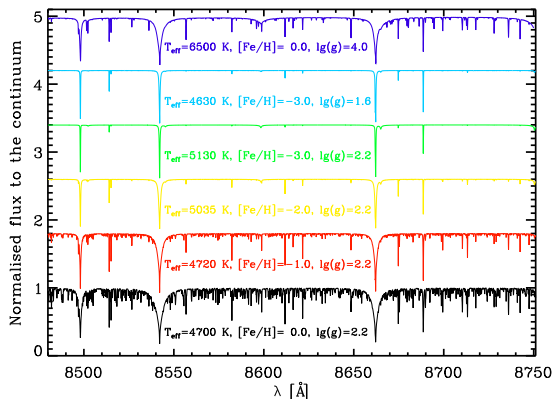


Figure 1. Spectra in the Gaia-RVS domain for the local simulations of Tab. 1. An offset has been added to the colored curves.

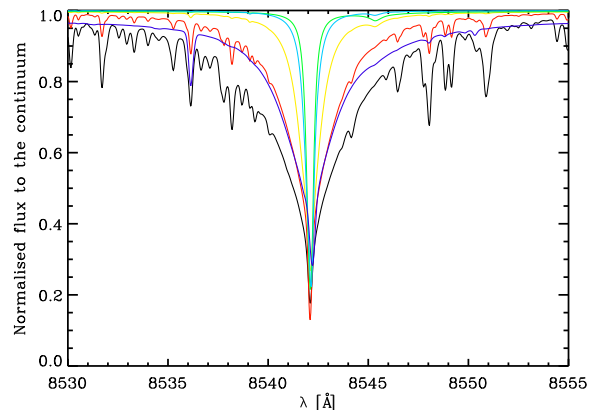


Figure 2. Enlargements of Fig. 1 around a Ca II line.

Tab. 1. Ramirez et al. [17] found that the sequence was long enough to ensure that the results were statistically significant and the comparison with observations is also very good. However, the other K giant models we haven't done any comparisons with observations yet.

Figures 1 and 2 show the results for the local simulations and Fig. 3 and 4 the results for the global ones. It is noticeable how the Ca II triplet ($\lambda = 8498.02, 8542.09, 8662.14 \text{ \AA}$) is well visible in all the stars, even at low metallicity.

Following the work of [18], we determined the position, the depth and the width of Ca II triplet and of 20 Fe I lines selected to be non blended lines and to cover the spectral domain of the RVS [19]. For this preliminary work, we fitted the absorption lines with a gaussian function. Figure 5 shows that Fe I are mostly blueshifted (except for few cases with low excitation

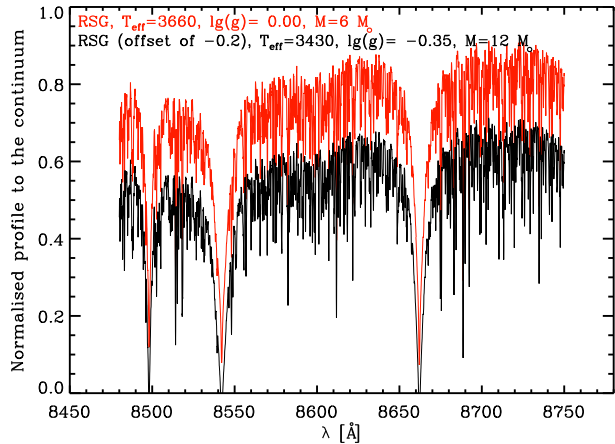


Figure 3. Spectra in the Gaia-RVS domain for the global simulations of Tab. 1.

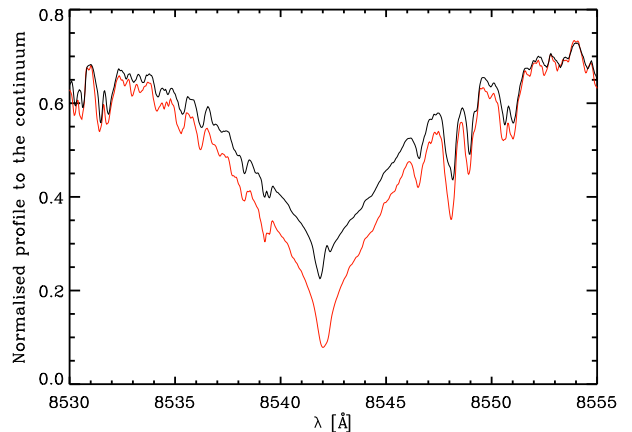


Figure 4. Enlargements of Fig. 3 around a Ca II line.

potential). The convective lineshift (Tab.1, $\Delta\lambda_{\text{FeI}}$) appears stronger for high excitation lines and it ranges, in average, from -0.22 km.s^{-1} (K giant with $[\text{Fe}/\text{H}]=-3.0$) to -0.75 km.s^{-1} (F star). The amplitude of the shift increases when going from K giants to the F star, as a consequence of the more vigorous convective motions. Moreover, the Ca II triplet lines are redshifted because these lines are formed in the upper part of the photosphere where the granulation pattern is reversed. The lineshift is particularly strong in the case of the F star (Tab.1, $\Delta\lambda_{\text{CaII}}$).

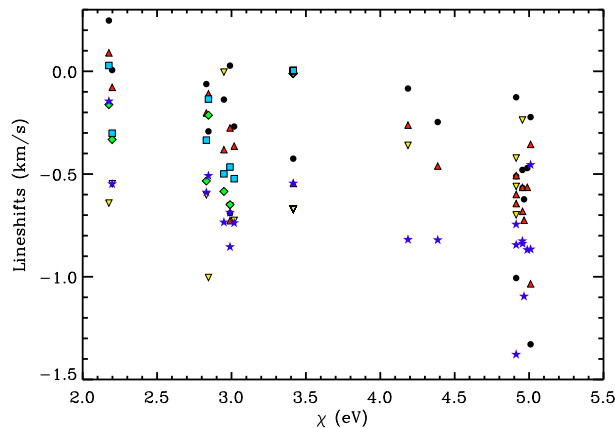


Figure 5. Convective shifts of 20 Fe I from [19] as a function of excitation potentials for local simulations of Tab. 1. For metalpoor stars, only visible lines in the spectra are reported.

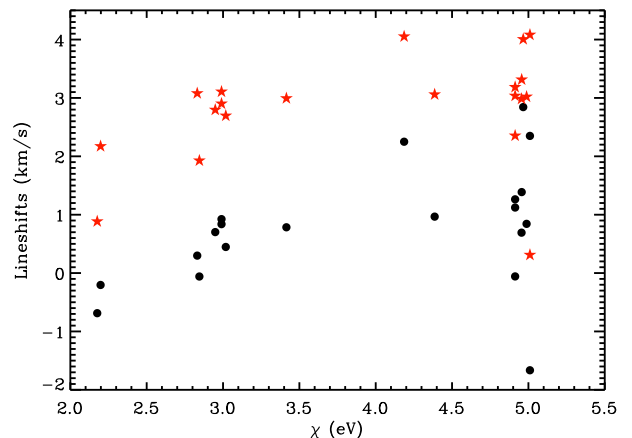


Figure 6. Convective shifts of 20 Fe I from [19] as a function of excitation potentials for global simulations of Tab. 1.

The lineshifts are not the same for all the lines in the RVS spectra. The precise amount of shift depends on the strength of the absorption line (and hence on the stellar metallicity), since different lines are formed at different atmospheric depths and thus experience different granulation contrasts and convective velocities. In fact, Fig. 7 displays that there is a correlation between lineshifts and line depth indicating that weaker line (high excitation potential) are in general more shifted than deep lines (low excitation potential). This picture is also supported by Fig. 5. In addition to this, Fig. 8 shows that there is not apparent connection with the line

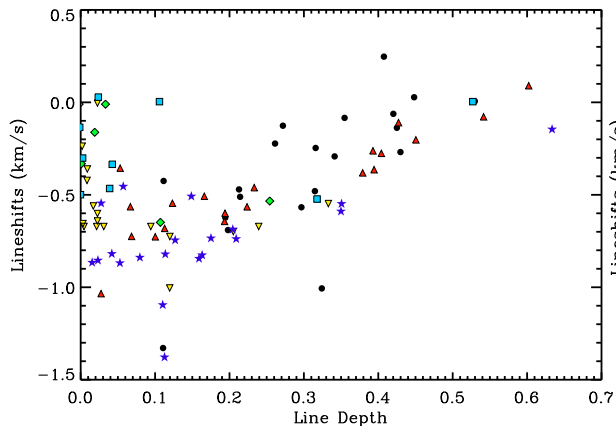


Figure 7. Same as in Fig. 5 but as a function of line depth.

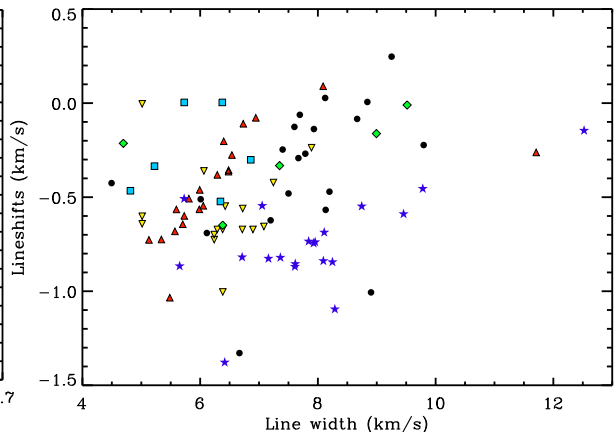


Figure 8. Same as in Fig. 5 but as a function of line width.

width as found by [20] for the Sun.

RSGs show a completely different behavior (Fig. 6) with strong redshifted Fe I up to 2.80 km.s^{-1} and blueshifted Ca II up to 8 km.s^{-1} (Tab.1). The reason is likely connected with the reversed-C shape of line bisectors observed by [21] on the prototypical RSG Betelgeuse and caused by a peculiar and vigorous convection but further investigations are needed and still in progress with RHD simulations.

In conclusion, velocity shifts of F and K giant stars are of the order of RVS accuracy ($\sim 1 \text{ km.s}^{-1}$), and they are even larger for RSG stars.

4. Photometric and photocentric variabilities and impact on parallaxes

Massive evolved stars like RSG stars give rise to large granules comparable to the stellar radius in the H and K bands, and an irregular pattern in the optical region [22]. These surface inhomogeneities vary with time and may affect strongly the photometric and astrometric measurements of Gaia.

Figure 9 displays the variability of a RSG during a period comparable with the Gaia mission in the blue and red photometric bands of Gaia. The photometric system of Gaia will be used to characterize the star's effective temperature, surface gravity and metallicity [23]. The simulations show fluctuations up to 0.28 mag in the blue and up to 0.15 mag in the red bands over 5 years. The photometric fluctuations of RSGs are not negligible and the uncertainties on $[\text{Fe}/\text{H}]$, T_{eff} and $\log g$ for these stars with $G < 15$ should be revised upwards for RSGs due to their convective motions [24].

The simulated surface of RSGs (Fig. 10) displays high-contrast structures with spots up to 50 times brighter than the dark ones with strong changes over some weeks. This aspect is connected with the underlying granulation pattern, but also with dynamical effects such as shocks and waves which dominate at optical depths smaller than 1 [22]. The convective-related surface structures in the Gaia G band affects strongly the position of the photocenter and cause temporal fluctuations (Fig. 11, left). The photocenter excursion is large, since it goes from 0.005 to 0.3 AU over 5 years of simulation and it is on average 0.132 AU (i.e., $\sim 3\%$ of the stellar radius). This value corresponds to a photocenter excursion of $\sim 10 \mu\text{as}$ for a star at 1 kpc, which

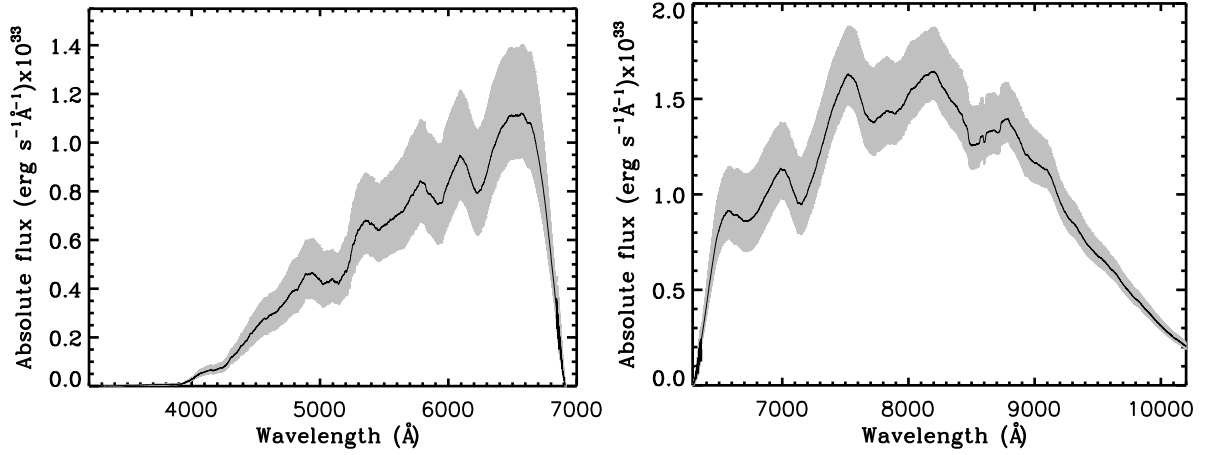


Figure 9. Spectral fluctuations in the blue (*left*) and red (*right*) Gaia photometric band [25] for a RSG simulation. The black curve is the average flux over ~ 5 years covered by the simulation, while the "grey shade" denotes the maximum and minimum fluctuations. The spectra have been smoothed to the Gaia photometric resolution of $R \sim 50$ [23]. Figures taken from [24].

is comparable to the Gaia accuracy of $\sim 10\mu\text{as}$ for stars brighter than 10.

Chiavassa et al. [24] calculated the Gaia parallax using Gaia Object Generator v7.0, GOG² [26] for RSGs with surface brightness asymmetries from RHD simulations (ϖ_{spot}) and without (ϖ). Figure 11 (right) shows that there is a systematic error of a few percent. This systematic error may be up to 15 times the formal error σ_{ϖ} [24]. Although this error should be used to revise σ_{ϖ} , there is little hope to be able to correct the Gaia parallaxes of RSGs from this parallax error, without knowing the run of the photocentric shift for each considered star. Thus, it might be of interest to monitor the photocentric deviations of a number of selected RSGs during the Gaia mission using interferometry and/or spectroscopy to obtain valuable information on the photocentric position and correct the resulting parallaxes using RHD predictions.

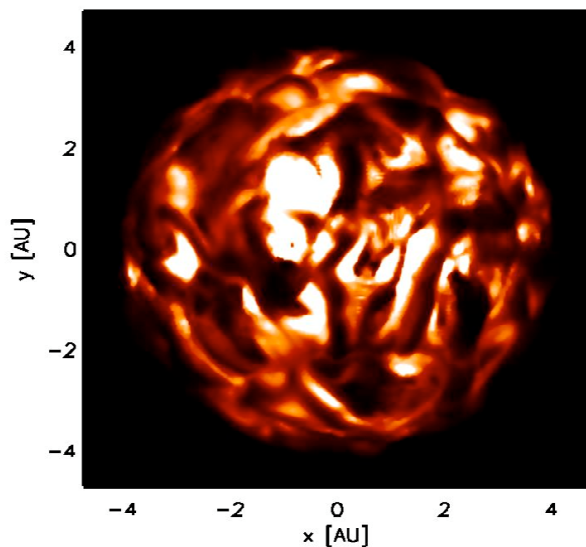


Figure 10. Synthetic map of intensity (the range is $[0 - 230000]$ $\text{erg/s/cm}^2/\text{\AA}$) in the Gaia G band [25]. Figure taken from [24].

² <http://gaia-gog.cnes.fr>

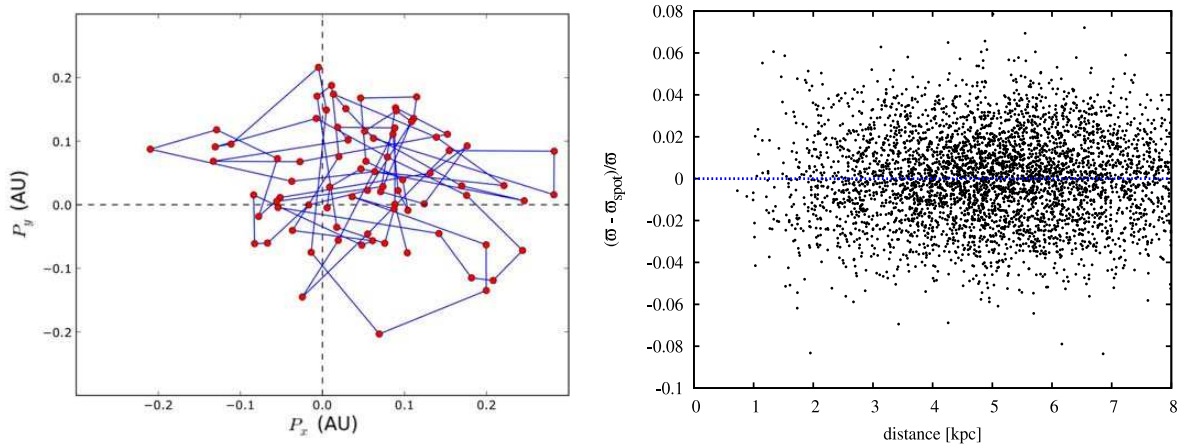


Figure 11. *Left:* photocenter displacement as a function of time for a RSG simulation. Each point is a snapshot 23 days apart for a total of 5 years of simulation (comparable to the duration of the Gaia mission). *Right:* relative difference between the parallaxes computed with and without the photocentric motion of the left panel, as a function of the distance. Figures taken from [24].

5. Conclusions and perspectives

3D hydrodynamical simulations of surface convection are a very important tool to account for convective shifts correction on the kinematic radial velocities, parallaxes and photometry.

With the increasing computer power, it is now possible to compute 3D model grids rather easily on reasonable timescale. In this framework, the 3D local model grid done with STAGGER-CODE (see contribution of Remo Collet in this Volume) will be available very soon together with the synthetic spectra in RVS domain (before Gaia launch date, mid 2013). The grid will include about 130 models with T_{eff} ranging from 4000 to 6500 K, $\log g$ from 1.5 to 5 and $[\text{Fe}/\text{H}] = 0.0, -1.0, -2.0, -3.0$. These models will not be enough to represent all the stars observed by Gaia and thus, following [16], we plan to apply 3D convective corrections to spectroscopic radial velocities obtained with less sophisticated models and templates.

Acknowledgments

The authors thank the Rechenzentrum Garching (RZG) for providing the computational resources necessary for this work.

References

- [1] Perryman M A C, de Boer K S, Gilmore G, Høg E, Lattanzi M G, Lindegren L, Luri X, Mignard F, Pace O and de Zeeuw P T 2001 *A&A* **369** 339–363 (*Preprint arXiv:astro-ph/0101235*)
- [2] Lindegren L, Babusiaux C, Bailer-Jones C, Bastian U, Brown A G A, Cropper M, Høg E, Jordi C, Katz D, van Leeuwen F, Luri X, Mignard F, de Bruijne J H J and Prusti T 2008 *A Giant Step: from Milli- to Micro-arcsecond Astrometry (IAU Symp. 248) (IAU Symposium vol 248)* ed W J Jin, I Platais, & M A C Perryman (Cambridge: Cambridge University Press) pp 217–223
- [3] Freytag B, Steffen M and Dorch B 2002 *Astronomische Nachrichten* **323** 213–219
- [4] Freytag B and Höfner S 2008 *A&A* **483** 571–583
- [5] Chiavassa A, Freytag B, Masseron T and Plez B 2011 *A&A* **535** A22 (*Preprint 1109.3619*)
- [6] Chiavassa A, Plez B, Josselin E and Freytag B 2009 *A&A* **506** 1351–1365 (*Preprint 0907.1860*)
- [7] Gustafsson B, Edvardsson B, Eriksson K, Jørgensen U G, Nordlund Å and Plez B 2008 *A&A* **486** 951–970 (*Preprint arXiv:0805.0554*)
- [8] Collet R, Asplund M and Trampedach R 2007 *A&A* **469** 687–706 (*Preprint arXiv:astro-ph/0703652*)

- [9] Collet R, Nordlund Å, Asplund M, Hayek W and Trampedach R 2009 *Memorie della Societa Astronomica Italiana* **80** 719+ (*Preprint* 0909.0690)
- [10] Collet R et al a *in preparation*
- [11] Katz D, Munari U, Cropper M, Zwitter T, Thévenin F, David M, Viala Y, Crifo F, Gomboc A, Royer F, Arenou F, Marrese P, Sordo R, Wilkinson M, Vallenari A, Turon C, Helmi A, Bono G, Perryman M, Gómez A, Tomasella L, Boschi F, Morin D, Haywood M, Soubiran C, Castelli F, Bijaoui A, Bertelli G, Prsa A, Mignot S, Sellier A, Baylac M O, Lebreton Y, Jauregi U, Siviero A, Bingham R, Chemla F, Coker J, Dibbens T, Hancock B, Holland A, Horville D, Huet J M, Laporte P, Melse T, Sayède F, Stevenson T J, Vola P, Walton D and Winter B 2004 *MNRAS* **354** 1223–1238 (*Preprint* arXiv:astro-ph/0409709)
- [12] Dravins D 1982 *ARA&A* **20** 61–89
- [13] Allende Prieto C, Lambert D L, Tull R G and MacQueen P J 2002 *ApJ* **566** L93–L96 (*Preprint* arXiv:astro-ph/0201355)
- [14] Lindegren L and Dravins D 2003 *A&A* **401** 1185–1201 (*Preprint* arXiv:astro-ph/0302522)
- [15] Allende Prieto C, Koesterke L, Ramírez I, Ludwig H G and Asplund M 2009 *Memorie della società astronomica italiana* **80** 622+ (*Preprint* 0909.0470)
- [16] Jasniewicz G, Crifo F, Soubiran C, Hestroffer D, Siebert A, Veltz L, Bigot L, Chemin L, David P, Guerrier A, Katz D, Ludwig H G, Richard P, Royer F, Sartoretti P and Udry S 2011 *EAS Publications Series (EAS Publications Series vol 45)* pp 195–200
- [17] Ramírez I, Collet R, Lambert D L, Allende Prieto C and Asplund M 2010 *ApJL* **725** L223–L227 (*Preprint* 1011.4077)
- [18] Bigot L and Thévenin F 2008 *SF2A-2008* ed C Charbonnel, F Combes, & R Samadi pp 3+–
- [19] Bigot L and Thévenin F 2006 *MNRAS* **372** 609–614
- [20] Asplund M, Nordlund Å, Trampedach R, Allende Prieto C and Stein R F 2000 *A&A* **359** 729–742 (*Preprint* arXiv:astro-ph/0005320)
- [21] Gray D F 2008 *AJ* **135** 1450–1458
- [22] Chiavassa A, Haubois X, Young J S, Plez B, Josselin E, Perrin G and Freytag B 2010 *A&A* **515** A12+ (*Preprint* 1003.1407)
- [23] Thévenin F 2008 *Physica Scripta Volume T* **133** 014010+–
- [24] Chiavassa A, Pasquato E, Jorissen A, Sacuto S, Babusiaux C, Freytag B, Ludwig H G, Cruzalèbes P, Rabbia Y, Spang A and Chesneau O 2011 *A&A* **528** A120+ (*Preprint* 1012.5234)
- [25] Jordi C, Gebran M, Carrasco J M, de Bruijne J, Voss H, Fabricius C, Knude J, Vallenari A, Kohley R and Mora A 2010 *A&A* **523** A48+ (*Preprint* 1008.0815)
- [26] Isasi Y, Figueras F, Luri X and Robin A C 2010 *Highlights of Spanish Astrophysics V* ed J M Diego, L J Goicoechea, J I González-Serrano, & J Gorgas pp 415+–

